Percolation through self-affine surfaces

1993 J. Phys. A: Math. Gen. 26 6115

(http://iopscience.iop.org/0305-4470/26/22/014)

J. Phys. A: Math. Gen. 26 (1993) 6115–6133. Printed in the UK

Percolation through self-affine surfaces

Jean Schmittbuhl†, Jean-Pierre Vilotte† and Stéphane Roux‡

† Laboratoire de Géologie, Ecole Normale Supérieure, 24 rue Lhomond, F-75231 Paris Cedex 05, France

‡ Laboratoire de Physique et Mécanique des Milieux Hétérogènes, Ecole Supérieure de Physique et Chimie Industrielles, 10 rue Vauquelin, F-75231 Paris Cedex 05, France

Received 17 May 1993

Abstract. We study the percolation transition in a longe-range correlated system: a self-affine surface. For all relevant physical cases (i.e. positive roughness exponents), it is found that the onset of percolation is governed by the largest wavelength of the height distribution, and thus self-averaging breaks down. Self-averaging is recovered for negative roughness exponents (i.e. power-law *decay* of the height pair correlation function) and, in this case, the critical exponents that characterize the transition are explicitly dependent on the roughness exponent above a threshold value. Below this threshold, the spatial correlations are no longer relevant. The problem is analytically investigated for a hierarchical network and by means of numerical simulations in two dimensions. Finally, we discuss the application of those properties to mercury porosimetry in cracks.

1. Introduction

While percolation theory has been extensively studied in the past decade [1], little attention has been paid to the occurrence of long-range spatial correlations [2, 3]. However, in natural systems spatial correlations are often observed and direct transposition of classical percolation theory can be misleading. Short-range correlations are expected to make the computation or the measurement of the percolation threshold explicitly dependent on the microstructure of the medium, but the critical behaviour is unaffected (i.e. still described by the usual critical exponents obtained in the absence of correlation). This illustrates the power of the concept of 'universality' and justifies the effort expended in the past on the determination of those exponents. For long-range correlations that picture is drasticaly changed as even the critical exponents may become different.

We shall address the question of the universality of the percolation transition in the presence of long-range correlations, with a special emphasis on the case of self-affine geometry. Self-affine geometry, which characterizes quite a number of different natural surfaces, exhibits such long-range correlations. Examples of the occurrence of such a property may be found in growth models [4], such as the boundary of Eden clusters or ballistic deposition models, landscape and erosion surfaces [5] or fracture surfaces [6–10]. Only recently has the importance of such long-range correlations in connection with percolation motivated some work [2, 3]

We proceed along the same lines, using different tools and techniques to generate correlated surfaces, and we extend the previous work to the case of self-affine surfaces which has never been addressed to our knowledge. We consider the case of a hierarchical lattice, which allows us to reach analytical conclusions. Then we use those results as a paradigm to numerically analyse the Euclidean case.

0305-4470/93/226115+19$07.50

The paper is organized as follow: first, a self-affine surface is constructed, both for Euclidean and hierarchical lattices, and the percolation transition is defined in section 2. In section 3 the influence of spatial correlations on the percolation transition is explicitly presented for the hierarchical lattice. The same problem is solved numerically in section 4 for the Euclidean case and the results are shown to be consistent with the hierarchical case. Finally, in section 5, the consequences of those results to mercury porosimetry applied to fractures are considered.

2. Self-affine surface construction

2.1. Euclidean lattice

A self-affine object is statistically invariant under an affine transformation: $x_i \rightarrow \lambda_i x_i$ for $i = 1, \ldots, d$ where d is the space dimension. Requiring that these transformations can be combined implies a group structure. As a consequence, each λ_i has to be an homogeneous function of one of them, say λ_1. The homogeneity exponents are called ζ_i: $\lambda_i = \lambda_1^{\zeta_i}$. The set of homogeneity indices, $\{\zeta_i\}$, characterizes the scaling properties of the self-affine object. We only consider here the case of surfaces with a mean plane parallel to $(x_1, \ldots, x_{d-1})$ along which the surface is isotropic. Therefore, $\zeta_i = 1$ for $i = 1, \ldots, d-1$. The only non-trivial exponent is thus relative to the scaling in the x_d direction—the 'height' of the surface—ζ_d, simply referred to as ζ in the following.

In order to illustrate the type of correlations introduced by a self-affine geometry we sketch the construction, introduced by Voss [11] (and presented in [4]), of a simple one-dimensional self-affine height profile $H(x)$.

The elementary process consists of knowing the values of H at both ends of a root segment, i and j, computing its value at the centre k as the average $(H_i + H_j)/2$ plus a fluctuation, h. At each generation m, the fluctuation h_m is picked from a statistical distribution $f(h)$ with zero mean. The magnitude of the fluctuation is scaled according to the length of the parent segment raised to the power ζ, ζ being the above-defined roughness exponent. The initial segment is supposed to be of length $L = 1$. We may choose f to be a Gaussian distribution although this is unessential. Let H_i be the height of a profile at point i. At the mth generation, by construction, 2^{m-1} new points will be generated and:

$$H_i = \tfrac{1}{2}(H_{i-l} + H_{i+l}) + 2^{-(m-1)\zeta} h_m(i) \tag{1}$$

where $l = 2^{-m}$ and $i = l, 3l, \ldots, (2m-1)l$. The height at a given point can finally be expressed, with this recursive construction, as the average of the two heights at the ends of the entire profile weighted by the distance to these points, plus a sum of fluctuations with different weights that depends on the precise location of each point. For positive ζ the amplitude of the fluctuations decreases exponentially with the generation. Therefore, after a few generations, the overall shape of the profile is roughly determined and the addition of the last points makes minor modifications to the profile, since the construction of the last heights is almost reduced to a linear interpolation between existing points. The statistical distribution of the heights H is then controlled by the fluctuation h_1 of the first generation. For negative ζ the final generations become dominant compared with the first and the 'memory effect' of the first generations is reduced. Figure 1(*a*) shows, for each point of the first generations, the location of the two parents' endpoints.

The two-dimensional construction follows the same basic iterative process. The main difference is in the dependence on the boundary conditions which are supposed to be periodic

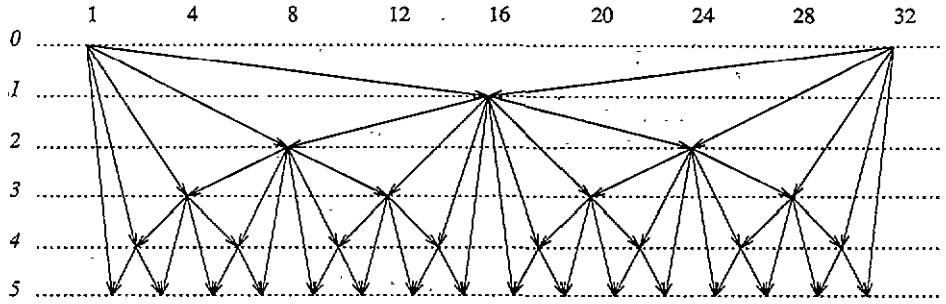

(*a*) Construction of a 1D euclidean self-affine profile

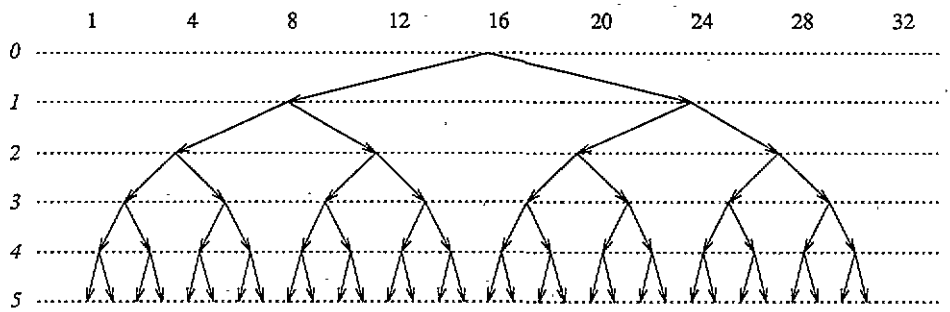

(*b*) Construction of a 1D hierarchical self-affine profile

Figure 1. Illustration of the construction of the self-affine profile in one dimension using two techniques presented in the text. (*a*) The first technique is the one which is used to generate the surfaces in two dimensions on a Euclidean lattice. (*b*) The second technique which is close to the previous one, albeit simpler, is tailored to the hierarchical lattice and is used in this context to reach an exact solution with this topology.

in both directions. At each step the height of the surface at the centre i of a square, with an initial height H_j at each of the vertices j, is computed as the average of the four vertex heights to which is added a random fluctuation, weighted by the length of the half diagonal raised to the power ζ. The initial state is a periodic square lattice, of size L, with a prescribed uniform height, say $H = 0$. At the first generation, the height at the centre of one square is generated which leads, using the periodicity, to a square lattice of mesh size $1/\sqrt{2}$ tilted at 45° from the original one. At the second generation, four new points, in one periodic cell, are generated and the process is iterated as many times as necessary. An example of such a surface is shown in figure 2(*a*) and a cut through the surface at the percolation threshold is displayed in figure 2(*b*). This construction has been used for the numerical simulations relative to the Euclidean lattice.

2.2. Hierarchical lattice

We now present an alternative way of generating a self-affine profile in one and two dimensions, perfectly suited to a hierarchical lattice, although not restricted to it.

Starting from a line segment with an initial uniform height, an additional height h_1 is added to each half of the parent segment. The heights h_1 are picked up randomly from a

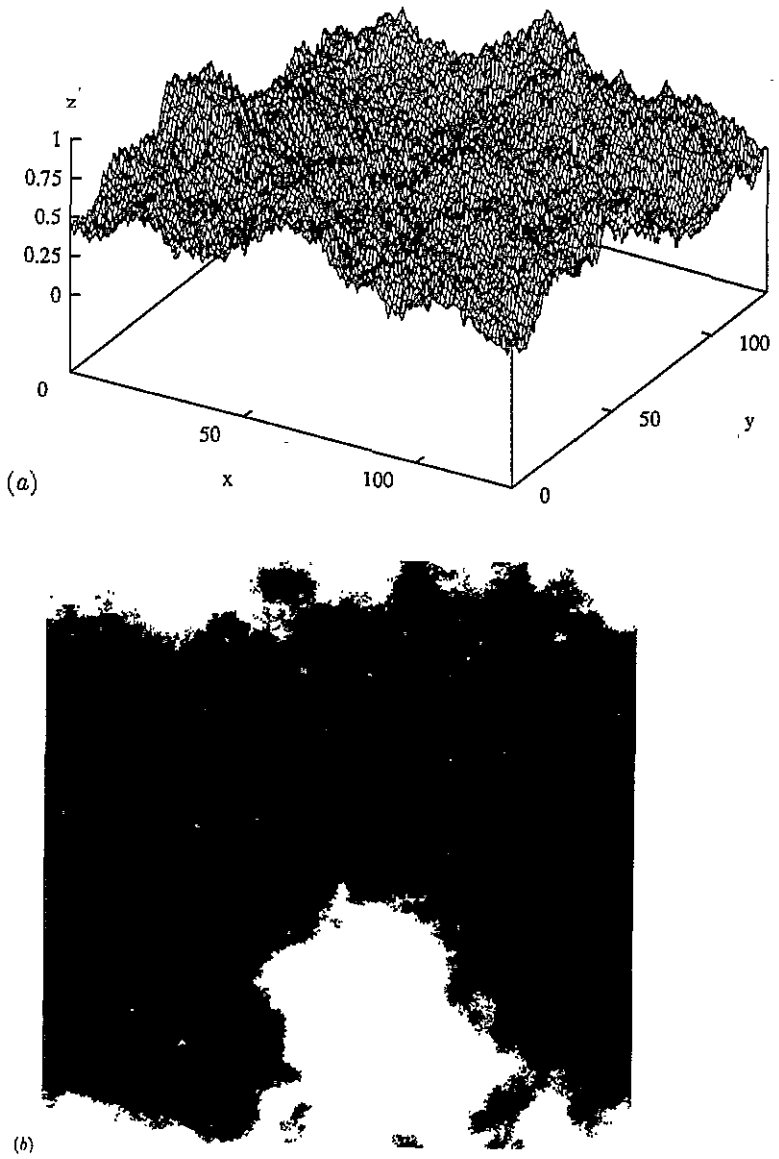

Figure 2. Shape of a 'natural' self-affine surface ($\zeta \approx 0.8$): (a) is a 3D plot of the surface where the average plane is parallel to (x; y); (b) a cut of the surface at the percolation threshold height. Black areas are below the threshold.

statistical distribution $f(h)$, with zero mean, and scaled by the length of the parent segment raised to the power ζ. This procedure is iterated again recursively until the desired length has been achieved. Initially (generation 0), the segment is of unit length and zero height. At each generation, the segment is divided by two and the number of segments after k generations is 2^k, with a length of 2^{-k}. Each segment can be considered as sites, and previous parent segments as 'macro-sites', in the spirit of a renormalization procedure. Figure 1(b) shows the construction of such profile and how the correlations develop. The simplicity of this tree-like structure allows us to compute the correlations in a straightforward manner. The first construction (figure 1(a)) shows that the tracking of correlations is much

more complex in the Euclidean case.

In two dimensions the construction is similar, using squares instead of line segments. A unit square with zero height is first divided in four equal squares to which independent additional heights h_1, picked from a statistical distribution $f(h)$ with zero mean, are prescribed. That procedure is iterated and at generation k the additional heights h_k are scaled by a factor $\lambda = 2^{-k\zeta}$. A general expression for the nth generation, of length 2^{-n} can be derived as

$$H_i = h_1 + \lambda h_2 + \lambda^2 h_3 + \ldots + \lambda^{n-1} h_n \tag{2}$$

where $\lambda = 2^{-\zeta}$.

This procedure is very close to, although simpler than, the previous case. It allows the computation of the correlation pair function of the height distribution. In that hierarchical construction, two sites i and j are correlated if they share a common ancestor. A natural distance, between the two sites i and j, can be defined as $d = (2^k - 1)2^{-n}$, with k being the number of generations by which the lattice must be coarse grained so that i and j share the same parent site†.

Let us now compute the correlation between the heights at two sites i and j. From generation 1 to $n - k$ the additional heights are identical for both sites i and j. For lower generations the two sites will belong to different squares and thus the additional heights they will be attributed will be uncorrelated. Thus the sum in (2) can be split in two parts:

$$H^i = X + Y \qquad H^j = X + Z \tag{3}$$

where Y and Z are uncorrelated and X is the height (as in (3)) truncated at order $n - k$. The correlation between the sites becomes

$$C = \langle H_i H_j \rangle - \langle H_i \rangle \langle H_j \rangle = \langle X^2 \rangle - \langle X \rangle^2 \tag{4}$$

i.e. equal to the variance of X: $1 + \lambda^2 + \ldots + \lambda^{2(n-1-m)} = (1 - \lambda^{2(n-k)})/(1 - \lambda^2)$ Two cases can be distinguished:

(i) When ζ is negative, or $\lambda \geqslant 1$, the correlation between the heights decays with the distance d as a power law;

$$C = \frac{\lambda^{2n}}{(\lambda^2 - 1)} [(2^n d + 1)^{-2\log(\lambda)/\log(2)} - \lambda^{-2n}] \tag{5}$$

thus

$$C \propto d^{2\zeta} \qquad \text{for} \qquad n \to \infty.$$

In such a case the reference to a self-affine geometry with a negative roughness exponent is rather awkward, since it is simply a power-law decay of the pair correlation function. However, it constitutes a natural extension of the following case which is our initial motivation for this study.

(ii) When ζ is positive, or $\lambda \leqslant 1$, the correlation amounts to

$$C = \frac{1}{1 - \lambda^2} (1 - (d + 2^{-n})^{-2\log(\lambda)/\log(2)}) \tag{6}$$

† We note *en passant* that this distance has the interesting feature of being an 'ultra-distance'. However, we will not use this property in the following.

or

$$C \propto (1 - d^{2\zeta}) \qquad \text{when} \qquad n \to \infty.$$

This represents the usual case of self-affine surfaces with a roughness exponent equal to $\zeta = -\log(\lambda)/\log(2)$.

If the distribution $f(h)$ is a Gaussian, then the height distribution $g(H)$ is a Gaussian since it is a sum of normal variables with various but fixed weights. In the same spirit, it is easy to show that for all distributions $f(h)$ with a finite second moment, and in the case $\lambda > 1$, $g(H)$ will tend toward a Gaussian distribution as n tends to infinity. On the contrary, for $\lambda < 1$, the final height distribution will keep the memory of the basic distribution f used to construct the profile, and it will not converge to a unique distribution. However, there is no need to specify the form of the distribution. We will see that the scaling properties of the percolation problem only depend on the parameter λ. In the following we will only assume that the average of $f(h)$ is 0 and the variance is 1.

Let us also note that depending on the the value of λ compared with 1, the width of the distribution of local heights will be either controlled by the large-scale roughness (i.e. h_1 in (2)), and thus independent of n (or of the number of sites) for λ smaller than 1, or imposed by the smaller length scale (i.e. h_n in (2)). In the latter case, the width of the distribution of heights will decrease exponentially with the generation of the lattice, as λ^n (or as a power law of the number of sites $(2^n)^{-\zeta}$). However, in order to compare the results for different system sizes, it is physically more relevant to deal with an overall distribution whose standard deviation is invariant. Therefore, for $\lambda > 1$, we propose to rescale all heights by a factor λ^{-n} so that the distribution of height no longer depends on n. In this case, we will introduce $\tilde{H}_i = \lambda^{-n} H_i$.

2.3. Percolation transition

Let us now define what we mean by percolation transition. In general, the percolation threshold p_c is defined on a regular infinite lattice as the value of the minimum concentration p of sites (or bonds) chosen at random and without correlations to form an infinite cluster with probability 1. Equivalently one could look for the existence of a continuous path of present sites which connects one border to the opposite one, in the thermodynamic limit of an infinite system size. A common way of choosing which sites are present or not involves attributing to each site a random number H picked from a distribution g and deciding that the site is present if H is less than a threshold ϕ so that

$$\int_{-\infty}^{\phi} g(H)\,\mathrm{d}H = p. \tag{7}$$

We will resort to the same procedure, but using for H the height of the surface, i.e. with the built-in correlations above described. Figure 2(*b*) shows a typical example of the percolation problem for the self-affine surface of figure 2(*a*).

In order to define the percolation transition it is important to introduce the notion of connectedness. On a Euclidean lattice one usually considers that only nearest neighbours are connected. On a hierarchical lattice a different choice is made for defining (connected) paths. For a one-generation lattice both lattices are equivalent. A 2×2 lattice will percolate if at least one of the two columns of two sites have both sites present. Above the first generation the percolation criterion is defined recursively: a lattice of generation n can be viewed as consisting of four sublattices of generation $n - 1$. It will percolate if it contains

at least two sublattices in series which themselves percolate. This definition is evidently tailored for real space renormalization through the identification of a percolating sublattice with a present (macro-)site. The definition of the hierarchical lattice together with the second construction (section 2.2) of the self-affine surface (which also fulfils the self-similarity) will lead us to an analytic solution of the percolation problem.

However, the critical exponents that can be computed exactly on this structure are known to be different from those relative to a Euclidean two-dimensional lattice. Nevertheless, the *relation between critical exponents are expected to be reliable* and thus can be transposed to the Euclidean lattice. This will allow us to test those predictions on the numerical results in the Euclidean case.

3. Percolation through a hierarchical lattice

3.1. Percolation formulation

We will first recall the analysis in the absence of correlation for the hierarchical lattice. Let p be the probability that a site is present. The probability that a lattice of generation 1 percolates when no correlation is present can be written as

$$P = \varphi(p) = 1 - (1 - p^2)^2. \tag{8}$$

Therefore in the absence of correlations, the percolation probability is obtained by iterating the function φ on the initial probability of site presence, $G(H) = \int_{-\infty}^{H} g(x)\,dx$. Moreover, this distribution is never used apart from the first step and thus we can simply express the threshold height $H_c = G^{(-1)}(p_c)$ using the inverse function of G.

This constitutes the basis for analysing usual percolation on this hierarchical network. Let us recall the most important results: the probability to percolate will converge for an infinite system size toward a step (Heavyside) distribution $P_\infty(p) = Y(p - p_c)$. The value of p_c is obtained as the non-trivial fixed point (different from 0 or 1) of φ (equation (8)), and thus satisfies $\varphi(p_c) = p_c$. A simple calculation leads to

$$p_c = \tfrac{1}{2}(\sqrt{5} - 1). \tag{9}$$

In the immediate vicinity of this fixed point the function φ is well behaved and the approach toward the fixed point can be obtained using a Taylor expansion of φ around p_c. If we introduce the local slope

$$a = \left.\frac{d\varphi(p)}{dp}\right|_{p=p_c} = 2(3 - \sqrt{5}) \tag{10}$$

we can write $\varphi(p) = p_c + a(p - p_c) + \mathcal{O}((p - p_c)^2)$. The width, σ_n, of the percolation probability distribution, $P_n(p) = \varphi^{(n)}(p)$, will asymptotically scale as $\sigma_n \propto a^{-n}$ or, using the system size as the number of points, $L = 2^n$, as

$$\sigma(L) \propto L^{-1/\nu} \tag{11}$$

where $\nu = \log(2)/\log(a) \approx 1.63$ is the so-called correlation length exponent. Indeed one can interpret such a scaling through the occurrence of a characteristic length scale ξ which diverges when the probability of presence p approaches p_c as $\xi \propto |p - p_c|^{-\nu}$.

Let us now introduce correlations in the height distribution. We consider the second contruction of a self-affine surface presented in the previous section.

From the construction of the surface it is possible to reformulate the procedure in the following way: a self-affine surface at generation n can be obtained from four independent surfaces at generation $(n-1)$ rescaled by a factor of two in the plane (x_1, x_2) as can be seen from (2). For each of the four $(n-1)$ lattices the initial height H_i' is given by

$$H_i' = h_2 + \lambda h_3 + \ldots + \lambda^{n-2} h_n. \tag{12}$$

In order to obtain (2) all heights H_i' should be rescaled by a factor λ and then each sublattice is independently to be translated as a block by a height h_1 randomly picked from the distribution $f(h)$. Then the four sublattices are pasted together to form a generation-n surface. For a site i which was part of a sublattice with a height H', the new height reads

$$H_i = h_1 + \lambda H' \tag{13}$$

which is similar to (2), using the expression of H_i' in (12).

We can now compute the recurrence on the probability to percolate. Let $P_n(\phi)$ be the probability that a generation-n surface, cut at a height $H = \phi$, contains a percolating path from one border to the opposite one. In order to relate P_n to P_{n-1}, we use the previous property. Cutting the generation-n surface at a level ϕ is equivalent to cutting each generation-$(n-1)$ surface at a level ϕ' with $\phi' = (\phi - h)/\lambda$. We now introduce the probability $\Pi_{n-1}(\phi)$ which takes into account the transformation on ϕ

$$\Pi_{n-1}(\phi) = \int_{-\infty}^{\infty} P_{n-1}((\phi - h)/\lambda) f(h)\, \mathrm{d}h. \tag{14}$$

The probability to percolate on the generation-n surface is written now as in the uncorrelated case,

$$P_n(\phi) = \varphi(\Pi_{n-1}(\phi)) \tag{15}$$

as in (8), since the latter equation only describes the peculiar topology of paths on the hierarchical lattice. Equations (14) and (15) constitute the recurrence we look for to study the scaling properties.

Equation (14) leads to simple relations between moments of the distributions P_n and Π_n. In particular, the variance of the distributions is important. We call σ_n^2 the variance of P_n and ς_n^2 that of Π_n. Both are related through

$$\varsigma_n^2 = \lambda^2 \sigma_n^2 + 1. \tag{16}$$

Let us now distinguish between the cases λ smaller or larger than 1.

3.2. Self-affine surface $\lambda < 1$ ($\zeta > 0$)

We need to complement (16) by the corresponding relation between σ_n and ς_{n-1} derived from (15). Unfortunately it is difficult to express such a relation in the general case. However, bounds can easily be obtained. Since φ is well behaved, one can establish the inequalities:

$$(\lambda^2 \sigma_{n-1}^2 + 1)/b^2 < \sigma_n^2 \leqslant (\lambda^2 \sigma_{n-1}^2 + 1) \tag{17}$$

where b is the maximum value of $\mathrm{d}\varphi(x)/\mathrm{d}x = 8/(3\sqrt{3})$. Thus σ_n is bounded from above and below by two convergent series having a finite non-zero limit. The upper series converges to $\sigma \to 1/\sqrt{1-\lambda^2}$, while the lower tends to $\sigma \to 1/\sqrt{b^2-\lambda^2}$.

In fact the upper bound is expected to give the correct behaviour. If we note that the height distribution will tend to have a width proportional to $(1-\lambda)^{-1/2}$, it is natural to express the scaling of the σ compared with the height distribution, or to introduce $\tilde{\sigma} = (1-\lambda)^{1/2}\sigma$. If we assume that the upper bound is valid, we obtain $\tilde{\sigma} \propto \sqrt{1-\lambda}$ in the neighbourhood of $\lambda = 1$ or $\zeta = 0$. The other bound gives a quicker vanishing of $\tilde{\sigma}$ as λ approaches 1.

Those bounds are sufficient to insure that the distribution will not tend toward a step function and thus self-averaging breaks down in this case. The additional details of the surface, which are given by increasing the number of points n, will play such a minor part that the percolation process, even for infinite n, will behave as if the system size was finite in the absence of correlation. We can also compare the result with a situation where an external field is imposed on the system giving rise to a finite correlation length. The genuine critical behaviour is then recovered for $\lambda = 1$. This result is rather surprising: *even in the thermodynamic limit, the percolation transition on a self-affine surface is only critical for a zero roughness exponent.*

3.3. *Long-range correlated surface* $\lambda > 1$ ($\zeta < 0$)

In order to derive (17) we made no assumption on the value of λ. Thus this inequality also holds for negative ζ. However, in this case we have already pointed out that the distribution of heights, $g(H)$, is now controlled by the smaller length scale of the surface, and thus the width of the distribution scales as λ^n. The larger the number of sites is, the wider the distribution g. In order to reach physical conclusions we should deal with rescaled heights $\tilde{H}_i = H_i\lambda^{-n}$. It is straightforward to rewrite the recursion relation for the scaled threshold $\tilde{\phi} = \phi\lambda^{-n}$

$$\tilde{\Pi}_{n-1}(\tilde{\phi}) = \int_{-\infty}^{\infty} \tilde{P}_{n-1}(\tilde{\phi} - h\lambda^{-n}) f(h)\,\mathrm{d}h \tag{18'}$$

$$\tilde{P}_n(\tilde{\phi}) = \varphi(\tilde{\Pi}_{n-1}(\tilde{\phi})) \tag{18''}$$

with obvious notation. The variance of the threshold distribution σ_n^2 is to be compared with the variance of g, and thus we introduce $\tilde{\sigma}_n = \sigma_n/\lambda^n$. The inequalities (17) expressed for $\tilde{\sigma}_n$ can be written

$$(\tilde{\sigma}_{n-1}^2 + \lambda^{-2n})/b^2 < \tilde{\sigma}_n^2 < (\tilde{\sigma}_{n-1}^2 + \lambda^{-2n}). \tag{19}$$

The upper bound is now finite while the lower bound is zero. The upper bound is very conservative and indeed, the variance of the distribution goes to zero as n tends to infinity.

The limit distribution $\tilde{P}_\infty$ when n goes to infinity should fulfil

$$\begin{aligned}\tilde{P}_\infty(\tilde{\phi}) &= \varphi\left(\int_{-\infty}^{\infty} \tilde{P}_\infty(\tilde{\phi} - h\lambda^{-n}) f(h)\,\mathrm{d}h\right) \\ &= \varphi(\tilde{P}_\infty(\tilde{\phi}))\end{aligned} \tag{20}$$

since $\lambda^{-n} \to 0$ as n goes to infinity. The distributions which fulfil this condition can only assume the values $P_\infty = 0$, p_c, or 1, the three fixed points of φ. The instability of the intermediate value p_c leads to 0 or 1 as the only possible values over a non-zero interval.

Since P_∞ is an increasing function, a step (Heavyside) distribution is the only possible limit: $P_\infty(\tilde{\phi}) = Y(\tilde{\phi} - \tilde{\phi}_c)$, as for the uncorrelated surface case.

Since the variance $\tilde{\sigma}_n$ converges to zero for large n, this allows to change the inequality (19) into a genuine equality

$$\tilde{\sigma}_n^2 = (\tilde{\sigma}_{n-1}^2 + \lambda^{-2n})/a^2 \tag{21}$$

for large n, with a given in (10). The asymptotic behaviour of $\tilde{\sigma}_n$ will be an exponential of n which we write $\tilde{\sigma}_n = x_n \mu^{-n}$ where the series x_n converge to a constant x_∞. Inserting this expression in (21) leads to

$$a^2 x_n^2 = \left(\mu^2 x_{n-1}^2 + (\lambda/\mu)^{-2n}\right). \tag{22}$$

To keep the series x_n bounded, μ has to be smaller than or equal to λ. Two cases have to be distinguished:

(i) $1 < \lambda < a$. In this case, $\mu = \lambda$. Equation (22) gives

$$x_\infty = \frac{1}{\sqrt{(a^2 - \lambda^2)}} \tag{23}$$

and thus $\tilde{\sigma}_n \sim \lambda^{-n} \sim L^{\zeta}$. Using the scaling result (11), we can write this result in the form of an effective correlation length exponent, ν_{eff}:

$$\nu_{\text{eff}} = -1/\zeta. \tag{24}$$

(ii) $a < \lambda$. In this case, the previous solution breaks down. Indeed, the result ($\mu = \lambda$) would imply that the reduction in the width of the distribution is faster than in the absence of correlation. This is obviously unphysical. In fact, μ is strictly smaller than λ so that the second term of (22) vanishes in the large n limit. Therefore, μ has to be equal to a. Thus, $\tilde{\sigma}_n \sim a^{-n}$ or

$$\nu_{\text{eff}} = \nu \tag{25}$$

where ν designates the standard percolation exponent, (10).

Figure 3 summarizes the above results. For ζ smaller than a threshold value $\zeta^* = -1/\nu \approx -0.613$, the correlation length exponent is identical to that of standard percolation. More generally, in this case, the universality class, i.e. all critical exponents are expected to be insensitive to the presence of correlations and they assume their usual value. For larger ζ, in contrast, the long-range correlations modify the universality class and, in particular, the correlation length exponent.

We have mentioned the fact that the numerical value of critical exponents obtained on the hierarchical lattice were not reliable, in the sense that they could not be directly compared with their Euclidean counterpart. However, *relations between exponents are expected to be preserved.* Therefore, from the result obtained on the hierarchical lattice, we propose the following behaviour

$$\nu_{\text{eff}} = \begin{cases} \infty & \text{if } \zeta > 0 \\ -1/\zeta & \text{if } -1/\nu < \zeta < 0 \\ \nu & \text{if } \zeta < -1/\nu \end{cases} \tag{26}$$

with ν equal to the standard percolation value. On the Euclidean lattice for $d = 2$, $\nu = 4/3$ and on a hierarchical lattice, $\nu \approx 1.63$. The ν_{eff} value for $\zeta > 0$ is here indicated as conventional. We have already mentioned the fact that this case is expected to lead to off-critical behaviour (i.e. it should behave as if the system size was finite). Let us now confront this prediction with the numerical simulations performed on the Euclidean lattice.

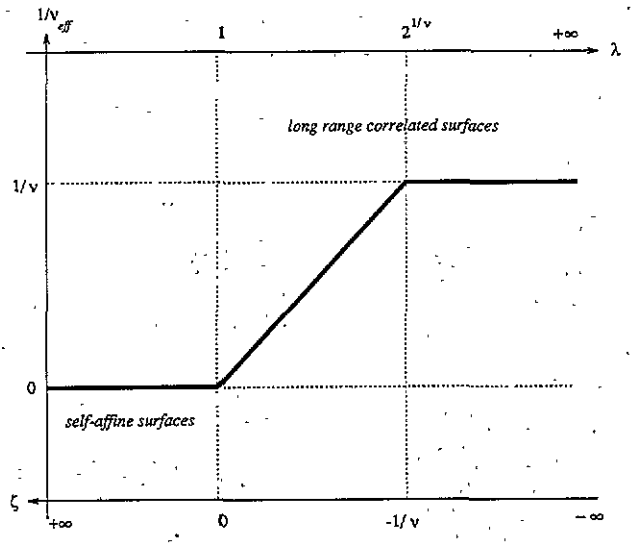

Figure 3. Evolution of $1/\nu_{\text{eff}}$ as a function of ζ. For small ζ the standard percolation case is recovered. Above ζ^*, but for negative roughness exponents, the correlation length exponent depends on ζ. Finally, for positive ζ, the length exponent vanishes. No critical point is obtained even in the thermodynamic limit.

4. Euclidean lattice

We now report the result of numerical simulations in the case of an Euclidean lattice with the construction of the surface presented in section 2. We have investigated ζ exponents equal to $-2, -1, -0.5, 0, 0.5, 0.8$ and 1. For each value of the roughness exponents we have generated 1000 independent surfaces for each size L (integer power of 2) ranging from 8 to 512. We checked for positive values of ζ that usual techniques for measuring the roughness exponent, when applied to the artificially generated surfaces, provided an estimate consistent with the chosen input exponent.

4.1. Percolation threshold

The percolation threshold is defined as mentioned in section 3. Numerically, we compute it for each surface by monitoring the height ϕ of the cutting plane. Starting from the interval $[H_{\min}, H_{\max}]$ which necessarily contains the effective threshold, we progressively reduce the size of the interval by a factor of 2, by checking if the surface percolates or not for a trial value of ϕ equal to the middle of the interval. This very simple procedure leads to a rapid convergence on the value of ϕ_c using simple tests. This dichotomy algorithm was continued to the desired accuracy (10^{-5}).

Figure 4 shows examples of surfaces generated using the first technique (Euclidean lattice case for four values of ζ). The surface is cut exactly at the threshold height, so that the black area is just above the percolation threshold (it contains one path of nearest-neighbour sites which is entirely contained in the black part). We note that for positive values of ζ and, in particular for the case which corresponds to real cracks ($\zeta \approx 0.8$), the black region is very compact and contains almost no hole. The first generation (large-scale) roughness is dominant and the last generations only bring minor alterations to the surface. As the roughness exponent is reduced the boundary of the black regions becomes

rougher and more diffuse. Finally, for $\zeta = -1$ correlations are hardly detectable by visual inspection. The same set of pictures using the second procedure (suited to the hierarchical lattice) described in section 2 are shown in figure 5. The same features are apparent. The most striking difference arises from the sharp discontinuities generated along the boundaries of large subsquares in the case of positive ζ exponent.

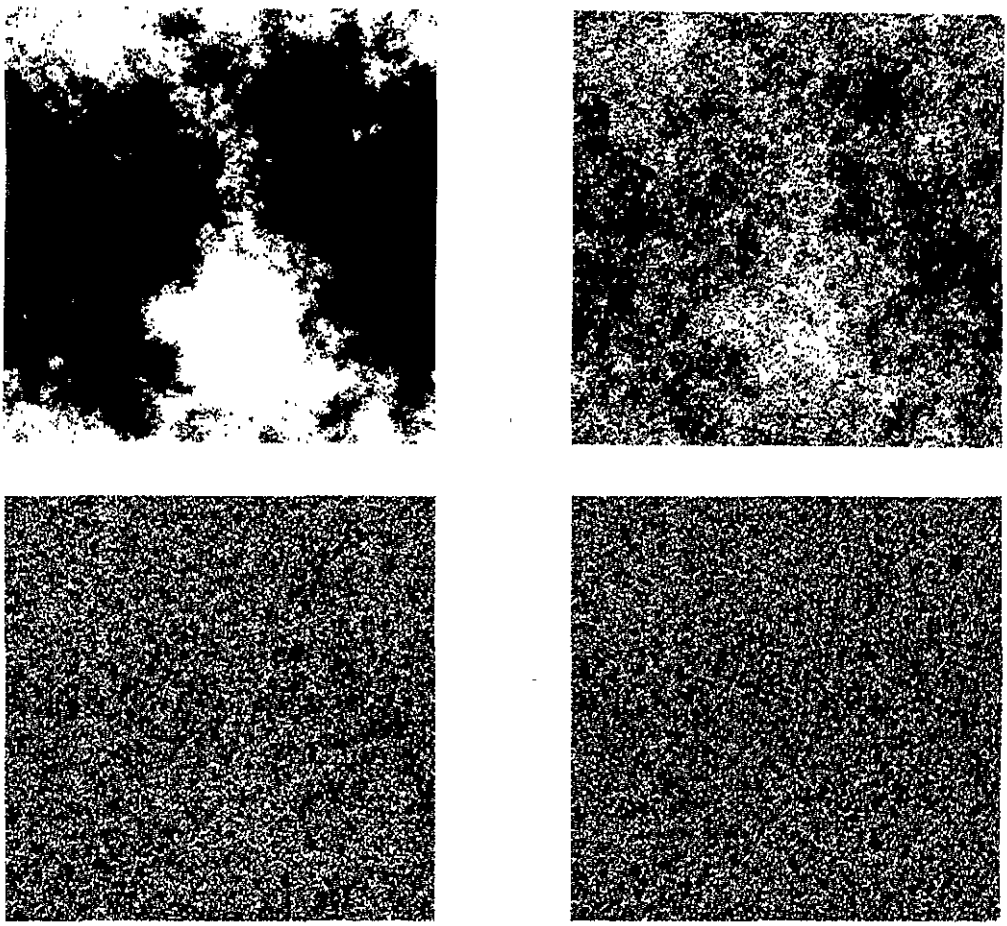

Figure 4. Four examples of the intersection of the surface with a constant height plane exactly at the percolation threshold. The four values of ζ considered are 0.5, 0, −0.5 and −1. The lattice size is 512. The construction used is that relative to Euclidean lattices.

The averaged percolation threshold $\phi_c(L, \zeta)$ for a finite-sized system is defined as

$$\phi_c(L, \zeta) = \int_{-\infty}^{\infty} \phi \frac{dP_n(\phi)}{d\phi} d\phi \tag{27}$$

where $L = 2^n$. When L tends to infinity the average percolation threshold tends to the asymptotic percolation threshold, when this notion can be defined without ambiguity (i.e. for positive ζ). Figure 6 shows $\phi_c(L, \zeta)$ as a function of L for various ζ values. We observe that the threshold decreases with ζ and that the size effects are very weak for positive ζ.

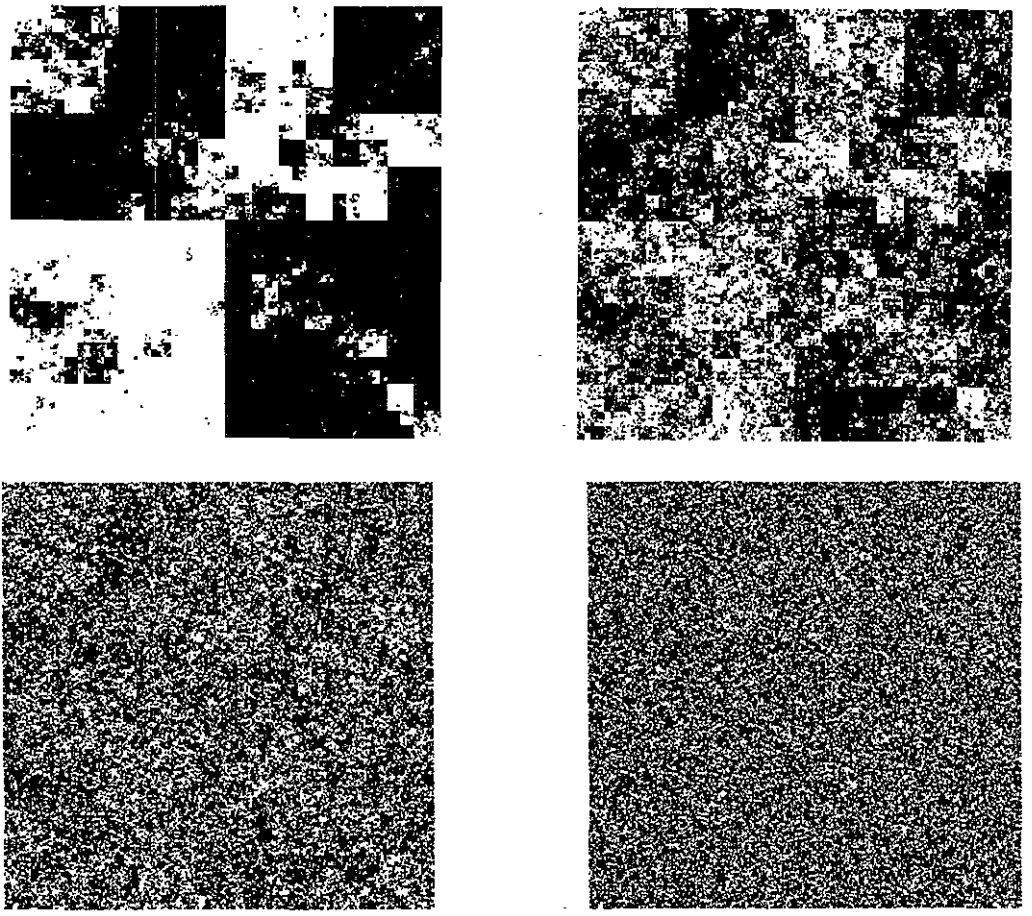

Figure 5. The same as figure 4 using the hierarchical lattice procedure to generate self-affine surfaces.

The variance of the distribution of threshold σ^2 is expected to behave as a power law of L with an exponent $-2/\nu_{\text{eff}}$, to be compared with the above predicted values (26). For positive values of ζ, we observe on figure 7 that the width of the distribution is nearly constant, in agreement with (26), or $\zeta = -0.5$, the expected law is $\sigma \propto L^{\zeta}$. The measured exponent is -0.3 ± 0.1 consistent with the predicted value. For $\zeta = -1$ and -2 we expect to recover the standard percolation case, $\sigma \propto L^{-3/4}$.

Figure 8 shows the entire threshold distribution for a positive value of the roughness exponent, $\zeta = 0.8$, and for three system sizes, $L = 8$, 32 and 512. We see on this graph that the size effect is extremely small and vanishes with L, in agreement with the expectation.

4.2. Incipient infinite cluster

We were also interested in other critical properties of the percolation problem on self-affine surfaces. In particular, the usual order parameter, defined as the probability that a site belongs to the infinite cluster. At the percolation threshold this is equivalent to studying the incipient infinite cluster. It can be seen from figures 4 and 5 that the structure of the infinite cluster is extremely dependent on the roughness exponent or the decay of long-range correlations.

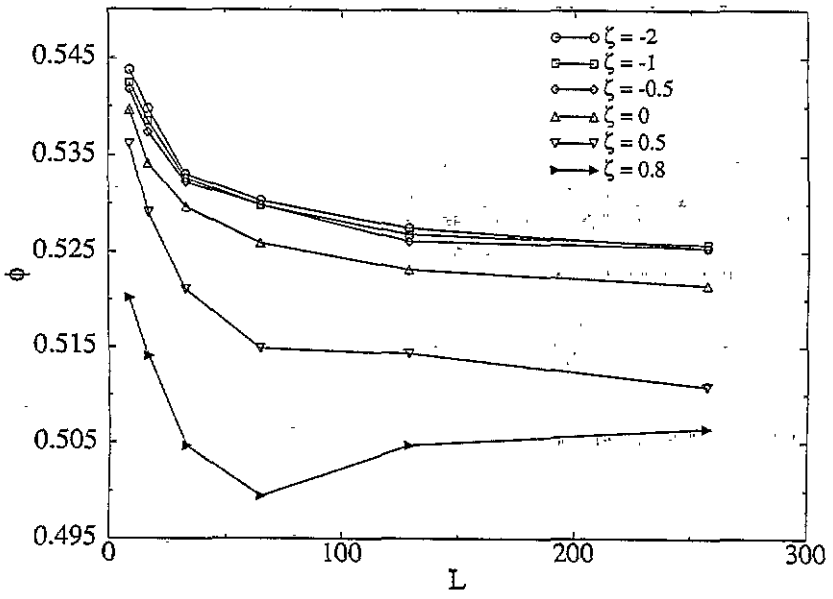

Figure 6. Average effective threshold $\phi_c(L, \zeta)$ as a function of L for various ζ values on the Euclidean lattice.

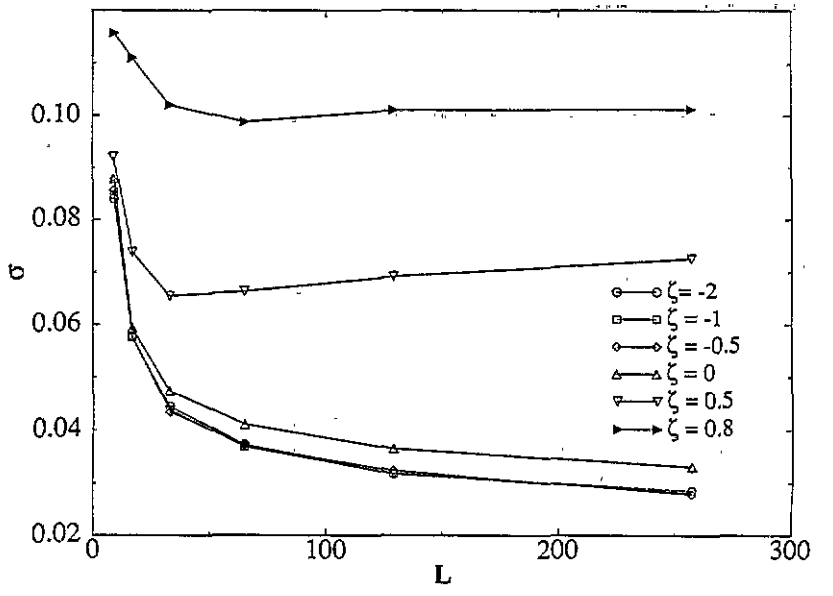

Figure 7. Standard deviation of the effective threshold distribution as a function of L for various ζ values on the Euclidean lattice. The data points are expected to follow asymptotically a power-law behaviour with an exponent $-1/\nu_{\text{eff}}$.

In standard percolation theory, the mass (i.e. number of sites) of the infinite cluster in a lattice of size L at the percolation threshold scales as $M \propto L^D$ where $D = d - \beta/\nu$, where d is the space dimension and β the order parameter critical exponent. In two dimensions

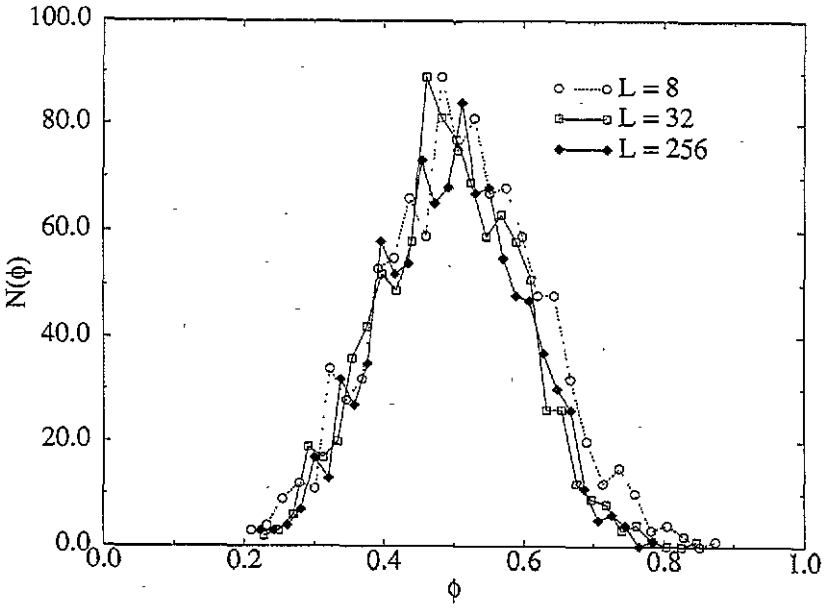

Figure 8. The entire threshold distribution for $\zeta = 0.8$ and for three system sizes, $L = 8$, 32 and 512.

$\beta = 5/36$ or $D \approx 1.89$.

We have plotted on figure 9, the density $d = M/L^2$ of the infinite cluster as a function of the system size, in a log–log scale, for various ζ exponents. For positive ζ, the density approaches a constant, again consistent with the fact that the finer details do not contribute more than marginally to the overall percolation properties. This is also consistent with the obvious guess that the clusters are compact, $D = d$, as can be seen, e.g., in figure 2(*b*). For $\zeta = -0.5$ the density seems to decrease slightly, with an estimate of the exponent equal to $(\beta/\nu)_{\text{eff}} \approx 0.1$ of the same order as the standard case $(\beta/\nu) \approx 0.11$. For smaller values of ζ, the expectation is that its value remains equal to the standard percolation value. The data are roughly consistent with this result although it is difficult to give a definitive answer due to the large fluctuations of the data.

4.3. Discussion

The results obtained for long-range correlations (i.e. $\zeta < 0$) can be compared with recent numerical [2] and analytical [3] results on correlated percolation, for which long-range spatial correlations are built with a different technique as: $\alpha \propto f(\mu) r^{-(d-\mu)}$ where d is the spatial dimension, r the distance and μ a tuning parameter.

The compactness of the incipient infinite cluster is shown to increase with long-range correlations and the cluster to become almost identical to its backbone [2]. This conclusion is mainly based on the evolution of the fractal dimension of the cluster backbone rather than on an evolution of the fractal dimension of the mass or density of the cluster itself. Indeed the size dependence of the density is shown to be quite constant for the limited range of correlations studied [2] and of the order of the standard percolation with an exponent $(\beta/\nu)_{\text{eff}} \approx 0.1$. That is consistent with our result for $\zeta < 0$. The results we have reported above are in agreement with this progressive increase of the compactness of the infinite cluster.

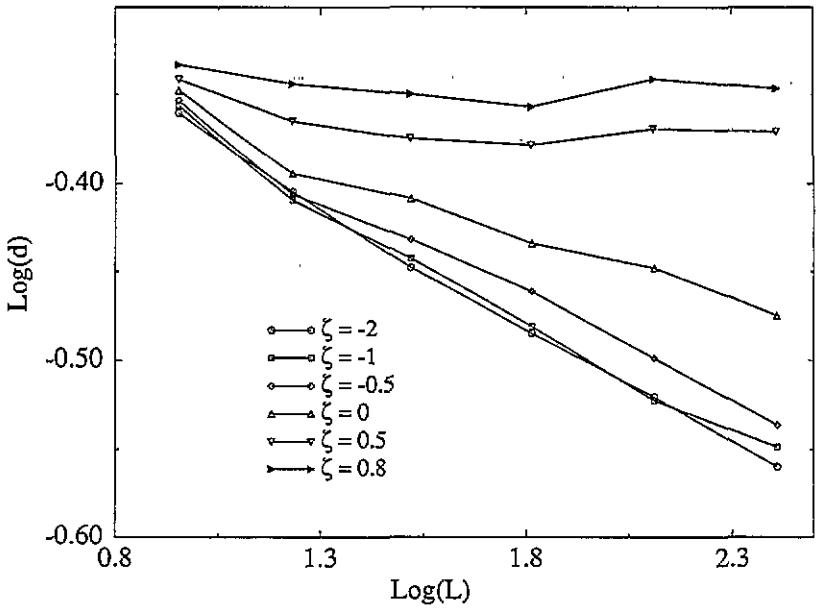

Figure 9. Density d of the incipient infinite cluster as a function of the system size L in log–log coordinates. We see that for positive ζ the density approaches a constant, whereas, for negative ζ, the density vanishes with the system size.

The variation of the correlation length exponent ν with the exponent ζ ($\zeta < 0$) is identical to the prediction obtained through an ϵ-expansion [3] and consistent with the numerical results reported in [2]. Indeed both studies predict the same variation of $\nu = 1/\zeta$ for ζ above a critical value ζ^*, with $\zeta^* \approx -3/4$ in [2] close to the critical value obtained in that study from the Euclidean lattice, i.e. $\zeta^* = 3/4$. That variation of ν leads to a singularity as $\zeta \to 0$ which is clearly observed [2, 3] and consistent with both our analytical and numerical results.

5. Application to mercury porosimetry

One of the most striking applications of percolation theory is to model the very slow drainage of a porous medium. In this case, where the capillary forces are dominant, the domain which is invaded by a non-wetting fluid being very slowly injected, can be compared with the infinite cluster connected to the injection side [12]. This is the origin of one algorithm known as the 'invasion percolation' which can be used to identify the infinite cluster without having to compute the threshold explicitly.

The justification of the model is as follows. With a given injection pressure p (and assuming that the pressure in the porous medium is zero), the meniscus of the non-wetting fluid will assume a curvature proportional to p. Thus pores the size of which is larger than this radius of curvature will be invaded provided they can be reached by the fluid. Smaller pores will be able to prevent the fluid from penetrating because of the high value of the capillary pressure. In a quasistatic invasion, with a constant flux, the fluid will invade the largest pore available along the interface.

The key point is the constraint that a site should be connected to the injection border by a continuous path of invaded pores in order to be invaded. Indeed if this constraint could be forgotten, then the invaded volume under a given pressure would genuinely give the cumulative pore volume of successive decreasing pore sizes. This is the important piece of information which is looked for when mercury invasion is used as a porosimetry analysing tool.

However, one can easily be convinced that the accessibility contraint is not always innocuous. Indeed, at the very beginning of the invasion, very few pores are accessible and thus the invaded volume is not representative of the set of pores in a given size class. At the end of the process on the contrary, most resistant sites will be located on the boundary of invaded regions and thus the invaded volume can be considered as reliable information. One can proceed more quantitatively along those lines so as to establish that once the invaded cluster spans the medium ('breakthrough' pressure), one can assume that most pores are accessible. Therefore, by recording the pressure–volume (p–v) characteristic, one can directly read the pore-size distribution, the volume of pores in a given size range. This principle is the basis of the widely used technique known as 'mercury porosimetry' to measure the pore-size distribution of a porous medium.

We mentioned in the introduction that the surface of cracks is self-affine, with a roughness exponent ζ close to 0.85. We have just seen that the percolation properties of such correlated surfaces were drastically different from those of usual percolation. Thus a natural point to explore is the consequences of this fact on the applicability of a mercury porosimetry measurement applied to a particular porous medium, an open crack.

What has been called a height up to this point throughout the paper is now to be considered as the aperture of the crack. The threshold level, ϕ, is the minimum aperture that can be invaded for a given pressure.

In particular, for a given pressure, one can compare the real invaded volume V_i, with the total volume, V_a, that would be invaded if all sites were connected to the inlet. V_i is the experimentally accessible measurement and V_a is the ideal information one would like to retrieve.

$$V_a = \int_{\phi}^{\infty} Hg(H)\,\mathrm{d}H. \tag{28}$$

We also introduce the total volume, $V_t = V_a(\phi = 0)$.

If no correlations are present, below the breakthrough pressure, the ratio $v = V_i/V_a$ tends to zero for a system of infinite size. Above the breakthrough pressure this ratio approaches one for very small threshold aperture ϕ, or a very large pressure. In order to use the measurement, one implicitly assumes that $v = 1$ and thus only pressures above the breakthrough pressure can be exploited.

We have computed the average value of the ratio v as a function of V_a/V_t for some values of ζ. The results are shown on figure 10. It shows a marked difference between self-affine and uncorrelated surfaces. Even for a very low pressure, i.e. from the very beginning of the injection, the ratio v is far from being zero. Therefore, one can extract meaningful (although underestimated) information even before the breakthrough pressure, in marked contrast with the uncorrelated case. On the other hand, the ratio approaches one very slowly, and thus the distribution may be less precisely measured than in the uncorrelated case just above the breakthrough point. We also note that as ζ is progressively decreased, the evolution of the ratio v with the accessible volume approaches the standard percolation case, expected to be achieved for $\zeta < -1/\nu$.

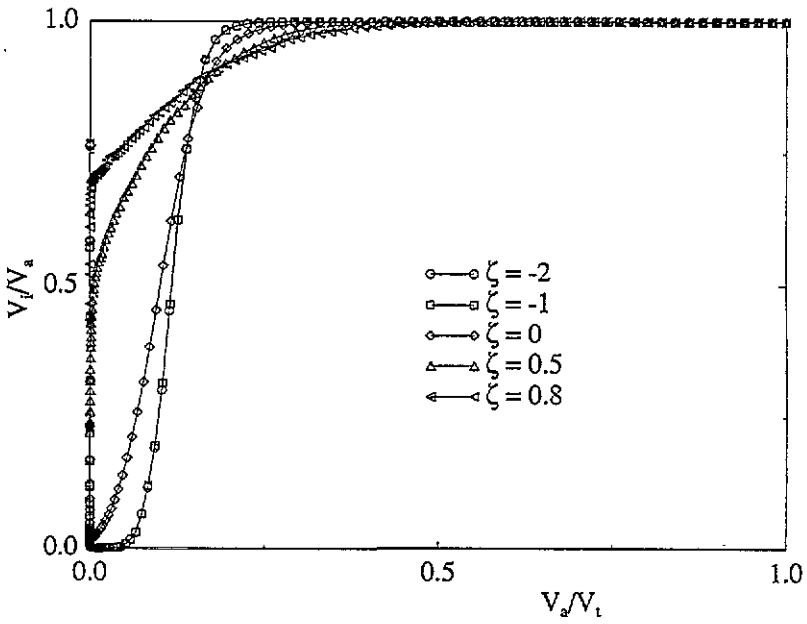

Figure 10. Relative invaded volume compared with the accessible one $v = V_i/V_a$, as a function of V_a/V_{Pt}. We see a marked difference of behaviour between positive and negative ζ exponents.

This observation is consistent with the previous discussion on percolation behaviour. For self-affine surfaces the breakthrough point is not a sharp transition and at this point a large volume has already been invaded. The interface with the rest of the system is nevertheless rather limited and thus the accessibility constraint never disappears completely. In contrast, for uncorrelated surfaces, at the breakthrough point, a fractal (ramified) cluster has been invaded with a vanishing volume and thus v is equal to zero for a system of infinite size. However, even if the invaded volume is small, it is widely spread in the system, and allows for a large interface with other pores, and hence this explains the sharp increase of v above the breakthrough pressure. It should also be noted that the very concept of the pore-size distribution has only a limited interest in the case of a long-range correlated surface, if correlations are not studied independently. In particular the connection with permeability is not direct and the scaling properties of the latter have to be independently determined (average value and fluctuations).

6. Conclusion

We have investigated the percolation behaviour both for a hierarchical network, using an analytic approach, and for a Euclidean lattice, through numerical simulations. Our main conclusion is that for self-affine surfaces ($\zeta > 0$), the percolation process does not show a genuine phase transition but rather behaves as a finite-size system, or as if an external field was imposed. For a long-range correlated surface with an exponent larger than $\zeta > -1/\nu$, then the percolation transition is well behaved, but it belongs to a different universality class from that for standard percolation, with critical exponents varying continuously with ζ. Finally, when the exponent ζ is smaller than $1/\nu$, the standard percolation problem is

recovered, and correlations do not change the universality class of the problem. Numerical simulations support this picture in two dimensions.

Finally, the applicability of mercury porosimetry has been investigated and was shown to lead to more reliable behaviour for low pressures and to a very slow convergence for large pressures. Experimental investigations of the latter process are clearly of interest.

Acknowledgments

We acknowledge useful discussions with L de Arcangelis, A Coniglio, A Hansen, J P Hulin and M Rosen. We thank S Prakash for communicating [3] prior to publication. The support of the GdR 'Physique des Milieux Hétérogènes Complexes' is acknowledged.

References

[1] Stauffer D1985 *Introduction to Percolation Theory* (London: Taylor and Francis)
[2] Prakash S, Havlin S, Schwartz M and Stanley H E 1992 *Phys. Rev.* A **46** 1724
[3] Weinrib A and Halperin B I 1984 *Phys. Rev.* B **29** 387
[4] Feder J 1988 *Fractals* (New York: Plenum)
Vicsek T 1989 *Fractal Growth Phenomena* (Singapore: World Science)
Family F and Visek T (ed) 1990 *Dynamics of Self-affine Surfaces* (Singapore: World Scientific)
[5] Newmann W I and Turcotte D L 1990 *Geophys. J. Int.* **100** 433
[6] Mandelbrot B B, Passoja D E and Paullay A J 1984 *Nature* **308** 721
[7] Brown S R and Sholz C H 1985 *J. Geol. Res.* **90** 5531
[8] Bouchaud E, Lapasset G and Planés J 1990 *Europhys. Lett.* **13** 73
[9] Schmittbuhl J, Gentier S and Roux S 1993 *Geophys. Res. Lett.* **20** 639
[10] Hansen A, Hinrichsen E L and Roux S 1991 *Phys. Rev. Lett.* **66** 2476
Måløy K J, Hansen A, Hinrichsen E L and Roux S 1992 *Phys. Rev. Lett.* **68** 213
[11] Voss R F 1985 *Fundamental Algorithms in Computer Graphics* ed R A Earnshaw (Berlin: Springer) pp 805–35
[12] Chandler R, Koplik J, Lerman K and Willemsen J F 1982 *J. Fluid Mech.* **119** 249